Characterizing the Electric Field Coupling from IC Heatsink Structures to External Cables Using TEM Cell Measurements

Shaowei Deng, Todd Hubing, *Fellow, IEEE*, and Daryl G. Beetner, *Senior Member, IEEE*

***Abstract*—One method for evaluating the unintentional radiated emissions from integrated circuits (ICs) involves mounting the IC on a printed circuit board (PCB) embedded in the wall of a transverse electromagnetic (TEM) cell. The signal voltages on the IC and its package produce electric fields that can couple to cables and other structures attached to the PCB, inducing common-mode currents that can be a primary source of unintentional radiated emissions. The signal currents in the IC and its package produce magnetic fields that can also result in common-mode currents on larger radiating structures. This paper describes a TEM cell measurement method employing a hybrid to separate the electric field coupling and the magnetic field coupling. The results of this measurement can be used to determine the product of the IC's self-capacitance and the effective voltage that drives this capacitance. This voltage–capacitance product characterizes the IC's ability to drive common-mode currents onto cables or enclosures due to electric field coupling. This information can then be used to estimate the resulting radiated emissions.**

***Index Terms*—Closed-form equation, mutual capacitance, radiated emissions, self-capacitance, transverse electromagnetic (TEM) cell.**

I. Introduction

THE TWIN standards SAE J1752/3 [1] and IEC 61967–2 [2] describe procedures for evaluating the radiated and conducted emissions of integrated circuits (ICs) using a transverse electromagnetic (TEM) cell. These procedures require an IC to be mounted on a 10 cm $\times$ 10 cm printed circuit board (PCB) with the IC on one side and the other components needed to exercise the IC on the other side. The PCB is mounted on the top side of a TEM cell with the IC side facing into the cell, as shown in Fig. 1. The voltage measured on one end of the cell is used to evaluate the performance of the IC from 150 kHz to 1 GHz. However, the procedure described in these standards does not directly measure the radiated emissions from the IC or its package. The voltage obtained is a function of the electric and magnetic field coupling between the IC test board and the TEM cell. The electric field coupling can be isolated from the magnetic field coupling by using a hybrid measurement setup as shown in Fig. 2 [3], [4]. The sum of the output voltages from both ends of the cell is proportional to the electric field coupling (or mutual capacitance) between the IC and the septum. The difference between the output voltages is proportional to the magnetic field coupling (or mutual inductance) between the IC current paths and the loop formed by the septum and TEM cell wall.

When the IC is mounted in a real product, the electric and magnetic field coupling can induce common-mode currents on cables and other large structures. These currents can be a primary source of unintentional radiated emissions. Magnetic field coupling is often referred to as being *current driven*, and electric field coupling is referred to as being *voltage driven*. Several studies of current-driven mechanisms have been presented in the literature [5]–[8]. However, the most significant coupling from ICs with large heatsinks is often voltage driven.

The voltage-driven mechanism for a simple microstrip trace coupling to a cable attached to a PCB is shown in Fig. 3. In this figure, V_{DM} represents the actual signal voltage on a trace or heatsink, and V_{CM} represents the effective common-mode voltage developed between the PCB and an attached cable. The amplitude of the equivalent common-mode voltage source V_{CM} is proportional to the self-capacitance of the trace or heatsink C_{trace} and can be used to estimate the radiated emissions from the board and the attached cables [9]. The parameters V_{DM} and C_{trace} characterize the electric field coupling between an IC driving a trace or heatsink and the objects off the board. The value of C_{trace} can be calculated by using three-dimensional numerical modeling tools when the geometry is well known. This paper will show that the product of V_{DM} and C_{trace} can be determined by TEM cell measurements. This enables TEM cell measurements of ICs or other components to be used to derive simple equivalent sources that can replace complex geometry descriptions in a full-wave analysis of the radiated emissions in order to estimate the peak radiated emissions.

The paper is organized as follows. In Section II, the electric field coupling from a microstrip trace to a TEM cell is described. The measured mutual capacitance results are compared with calculated results using numerical simulation tools for various trace geometries. In Section III, a closed-form equation for estimating the self-capacitance C_{trace} of a microstrip trace structure from measured values of the mutual capacitance between the TEM cell septum and trace C_{TEM} is derived. The closed-form estimates are compared with calculated results obtained by using an electrostatic field solver. Section IV demonstrates that for a small heatsink over a test board, the

Manuscript received January 14, 2007; revised June 3, 2007.

S. Deng was with the University of Missouri–Rolla, Rolla, MO 65409 USA. He is now with Juniper Networks, Sunnyvale, CA 94089 USA (e-mail: sdeng@juniper.net).

T. Hubing is with Clemson University, Clemson, SC 29634 USA (e-mail: hubing@clemson.edu).

D. G. Beetner is with the University of Missouri–Rolla, Rolla, MO 65409 USA (e-mail: beetner@umr.edu).

Color versions of one or more of the figures in this paper are available online at http://ieeexplore.ieee.org.

Digital Object Identifier 10.1109/TEMC.2007.908825

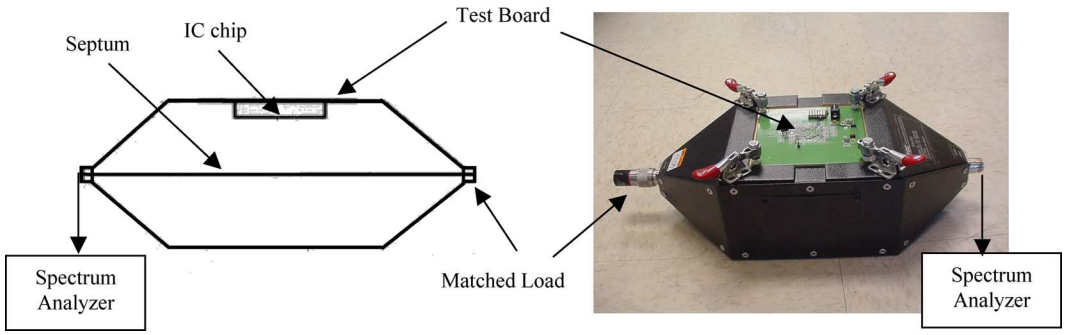

Fig. 1. Standard TEM cell measurement setup.

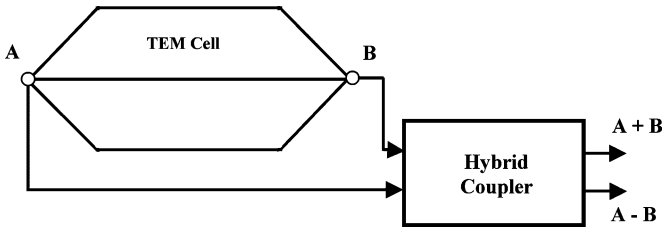

Fig. 2. TEM cell with hybrid coupler.

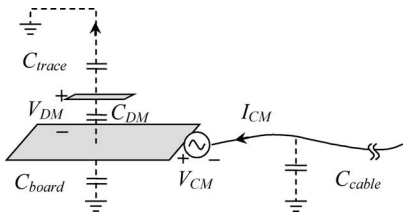

Fig. 3. Voltage-driven radiation mechanism.

measured mutual capacitance C_{TEM} can be used to estimate the heatsink self-capacitance. This section shows how TEM cell measurement results can be used to fully characterize the electric field coupling from an IC heatsink structure, resulting in a simple model that can be used to do a full-wave analysis of a complex geometry that includes the IC and heatsink. Section V summarizes the conclusions that can be drawn from the results presented here.

II. TEM Cell Mutual Capacitance Measurement

Fig. 4 illustrates the electric field coupling between a small patch of metal and the septum in a simple TEM cell test setup. A voltage difference between the patch and the wall of the TEM cell produces lines of electric flux that emanate from the patch. Most of these flux lines terminate on the wall of the TEM cell; however, a small portion of the flux lines terminate on the septum of the TEM cell. These flux lines produce a current in the septum that flows through the 50-Ω terminations at each end of the cell. In the hybrid setup (Fig. 2), the spectrum analyzer records the sum of the voltages induced at each end. The measured voltage is proportional to the voltage on the patch and is directly related to the ability of this patch to couple electric fields to moderately distant objects. It is convenient to represent the electric field coupling between the patch and the septum as

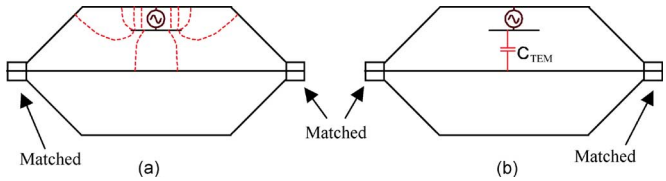

Fig. 4. Electric field coupling between a metal patch and a TEM cell.

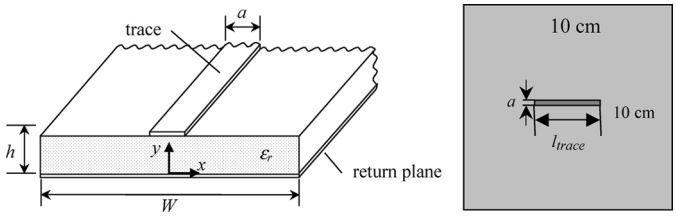

Fig. 5. Geometry of a microstrip trace with a finite-width return plane.

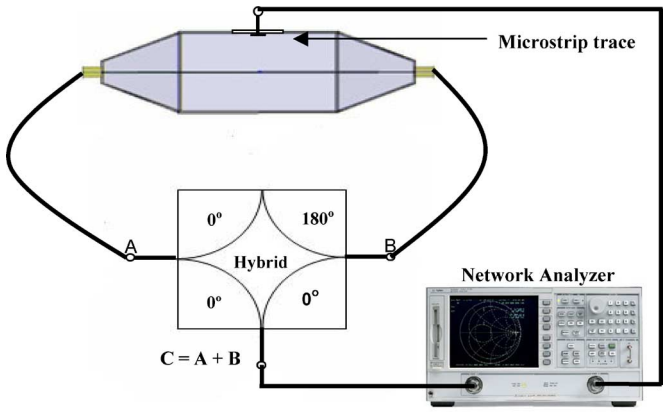

Fig. 6. Setup for TEM cell measurements.

a mutual capacitance C_{TEM} as indicated in Fig. 4. For a given TEM cell, the value of C_{TEM} is related to the geometry and the position of the patch.

A microstrip trace over a finite return plane is shown in Fig. 5. The mutual capacitances of six microstrip trace configurations were measured using the hybrid TEM cell setup presented in [3] and illustrated in Fig. 6. The six configurations are described in Table I. In these examples, the traces were located in the center of the test board. There was a dielectric substrate $(\varepsilon_r = 4.4)$ between each microstrip trace and the return plane. The distance

TABLE I
MEASURED AND NUMERICALLY CALCULATED MUTUAL CAPACITANCE (C_{TEM}) FOR MICROSTRIP TRACES IN TEM CELL

Trace Dimensions (mm)	$h = 0.8$ $a = 2$ $l_{trace} = 21$	$h = 1.6$ $a = 2$ $l_{trace} = 21$	$h = 2.4$ $a = 2$ $l_{trace} = 21$	$h = 0.8$ $a = 2$ $l_{trace} = 11$	$h = 1.6$ $a = 2$ $l_{trace} = 11$	$h = 2.4$ $a = 2$ $l_{trace} = 11$
Measured Result (fF)	14	17	21	8	9	13
Simulation Result (fF)	14.0	17.4	22.8	7.3	9.0	13.1

between the TEM cell wall and the septum was 4.5 cm. The trace-septum mutual capacitance for these configurations was obtained from the measured value of S_{21} and S_{11}, using [3]

$$C_{\mathrm{TEM}} = \mathrm{Re}\left\{\frac{1}{j50\pi f\left(\frac{1+S_{11}}{S_{21}}-1\right)}\right\}. \tag{1}$$

The electric field coupling from each of these open traces can be modeled fairly well with a single frequency-independent capacitance up to several hundred megahertz. The average value of the measured mutual capacitance from 30 to 500 MHz was recorded. The mutual capacitance for these trace configurations in the TEM cell was also calculated using a quasi-static field solver [10] that modeled the electric fields throughout the entire interior of the TEM cell. The measured mutual capacitance results and the simulation results are reported in Table I. The agreement between the measurements and the simulations is within 1 dB for all six trace configurations investigated.

III. CLOSED-FORM EQUATION FOR SELF-CAPACITANCE

The mutual capacitance between a trace and a return plane per unit length of a microstrip line is a function of the dielectric substrate relative permittivity, the trace width, the trace height, and the size of the return plane [11]. A closed-form equation for calculating the mutual capacitance between a trace and an infinitely large return plane (no dielectric substrate) is presented in [11] and [12]

$$C_{DM} = 2\pi\varepsilon_0\left\{\ln\left[\frac{F_1 h}{a}+\sqrt{1+\left(\frac{2h}{a}\right)^2}\right]\right\}^{-1} \tag{2}$$

where

$$F_1 = 6+(2\pi-6)\exp\left\{-\left(30.666\times\frac{h}{a}\right)^{0.7528}\right\}$$

and h is the height of the trace above the return plane, and a is the width of the microstrip trace. The self-capacitance of a microstrip trace with a finite return plane with or without a dielectric substrate can be estimated by using the closed-form approximate expression [13]

$$C_{\mathrm{trace}} = \frac{6.189}{\pi}\frac{h}{W}\frac{C_{DM}\, l_{\mathrm{trace}}}{\ln\left[1+3.845\left(\frac{L}{W}\right)\right]} \tag{3}$$

where C_{DM} is the mutual capacitance per unit length shown in (2), l_{trace} is the length of the trace, W is the width of the return plane, and L is the length of the return plane.

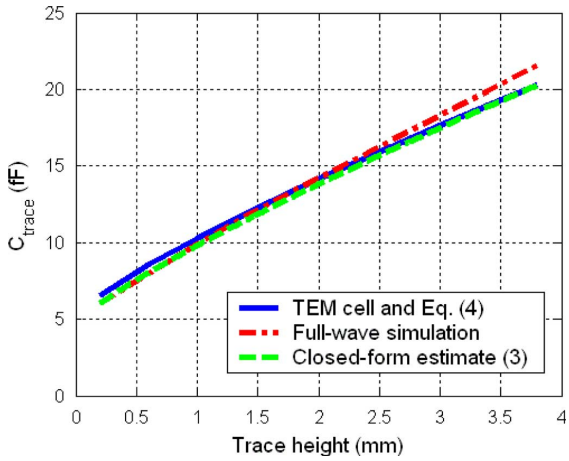

Fig. 7. Self-capacitance as a function of trace height h.

As described in Section II, C_{TEM} quantifies the electric field coupling between the microstrip trace and the septum. C_{TEM} is determined by the small portion of electric flux emanating from the trace and terminating on the septum of the TEM cell. For a given microstrip trace, it seems reasonable to expect the value of the trace self-capacitance C_{trace} (determined by the amount of flux originating on the trace and terminating at infinity) to be roughly proportional to the value of C_{TEM} (determined by the amount of flux that originates on the trace and terminates on the septum), provided that the distance to the septum is much greater than the trace height above the return plane.

This assumption was evaluated by comparing the calculated values of C_{TEM} with values of C_{trace} obtained using 3-D modeling software and the values obtained from the closed-form expression for C_{trace} shown in (3). The results demonstrated that C_{TEM} and C_{trace} were indeed proportional and related by a factor of 2.1 for this TEM cell geometry

$$C_{\mathrm{trace}} \approx \frac{C_{\mathrm{TEM}}}{2.1}. \tag{4}$$

Figs. 7–9 compare the estimated self-capacitance C_{trace}, calculated using the closed-form expression (4) and the quasi-static modeling code, to the results obtained by deriving C_{TEM} through simulation and estimating C_{trace} from (4). Fig. 7 plots C_{trace} for various trace heights (the trace width is 2 mm and the trace length is 21 mm). Fig. 8 plots C_{trace} for various trace widths (the trace height is 2.4 mm and trace length is 21 mm). Fig. 9 plots C_{trace} for various trace lengths (the trace width is 2 mm, and the trace height is 2.4 mm). For all the trace

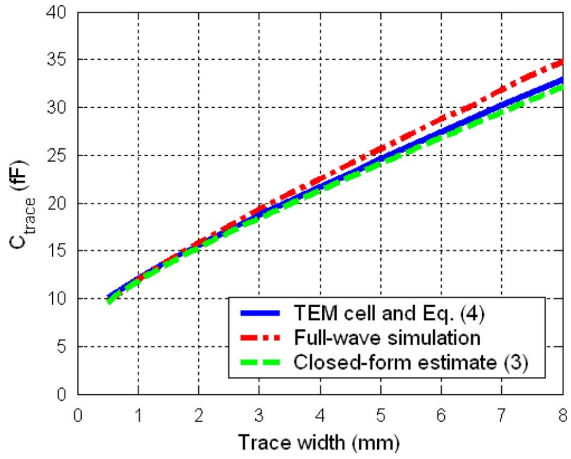

Fig. 8. Self-capacitance as a function of trace width a.

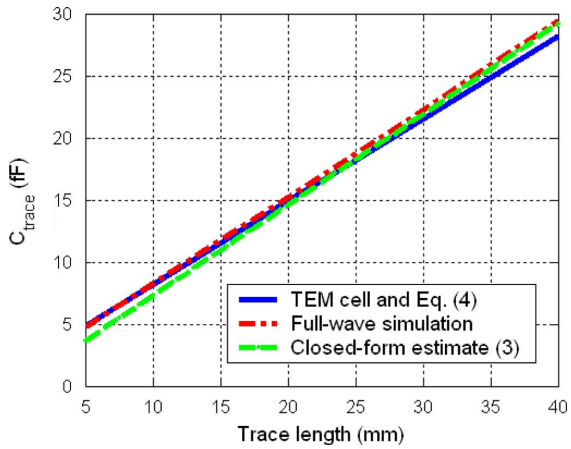

Fig. 9. Self-capacitance as a function of trace length, l.

geometries evaluated, the values of $C_{\rm trace}$ calculated using the three different methods agree within 2 dB.

As indicated in (3), the value of $C_{\rm trace}$ is also a function of the board dimensions. Measurements in the TEM cell, however, are performed by using a fixed-size 10 cm $\times$ 10 cm board. The self-capacitance of a microstrip trace mounted on boards of other sizes can be estimated by measuring the mutual capacitance of the trace on a TEM cell test board and correcting for the new board dimensions. From (3) and (4), we get

$$C_{\rm trace}(L,W) = C_{\rm trace}(L=0.1\ m, W=0.1\ m) \times \frac{0.1 \times \ln\left[1+3.845\left(\frac{0.1}{0.1}\right)\right]}{W \cdot \ln\left[1+3.845\left(\frac{L}{W}\right)\right]} \quad (5)$$

or

$$C_{\rm trace}(L,W) \approx \frac{C_{\rm TEM}}{2.1} \times \frac{0.158}{W \cdot \ln\left[1+3.845\left(\frac{L}{W}\right)\right]}. \quad (6)$$

Equation (6) can be used to estimate the self-capacitance of microstrip traces as long as they are not near the edge of the board. This equation relates the measured value $C_{\rm TEM}$ to the value $C_{\rm trace}$, which can be used to estimate the maximum radiated emissions due to voltage-driven common-mode currents [9]. The model in [9] shows that the electric field coupling is proportional to the product of the driving voltage and the trace capacitance. TEM cell measurements can be used to obtain this product directly, even when the voltage driving the trace is unknown. Since the TEM cell presents a 25-Ω load to the source/capacitor IC model, as illustrated in Fig. 10, the magnitude of the open-circuit voltage is given by

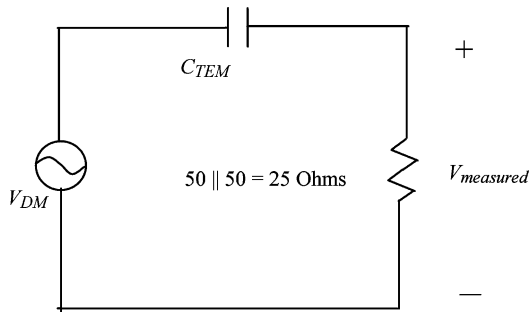

Fig. 10. Equivalent circuit showing TEM cell loading of the effective source structure.

$$|V_{DM}| = \frac{1+25\omega C_{\rm TEM}}{25\omega C_{\rm TEM}}|V_{\rm measured}| \approx \frac{|V_{\rm measured}|}{25\omega C_{\rm TEM}} \quad (7)$$

where V_{DM} is the open-circuit voltage on the trace, and $V_{\rm measured}$ is the voltage from the TEM cell measurement $(A+B)/2$ in Fig. 2. Rearranging the terms in (7), it is clear that the measured TEM cell voltage is proportional to the product of the voltage driving the trace and the quantity $C_{\rm TEM}$

$$|V_{\rm measured}| \approx 25\omega C_{\rm TEM}|V_{DM}|. \quad (8)$$

Note that by combining (4) and (8), a TEM cell measurement can be used to determine the product $C_{\rm trace}|V_{DM}|$. This product divided by the board's self-capacitance, is the amplitude of an equivalent common-mode voltage that can be placed between the board and the attached cables in full-wave simulations eliminating the need to model the traces or heatsinks explicitly [9]. In other words, this technique allows the TEM cell measurement results to be used to replace the complex structures on a circuit board in full-wave simulations.

IV. Heatsink Self-Capacitance and Radiated Emissions

A. Heatsink Self-Capacitance

Heatsinks can play a significant role in voltage-driven cable radiation. If a board is electrically small and the self-capacitance of the heatsink is smaller than that of the self-capacitance of the board, the model described in [9] and illustrated in Fig. 3 can be used to estimate the radiated emissions. The self-capacitance of the heatsink can be calculated using a numerical static field solver or determined from TEM cell mutual capacitance measurement results, as described in Section III for the microstrip trace.

A simple copper heatsink structure was constructed as shown in Fig. 11 and measured in a TEM cell, using the configuration shown in Fig. 6. The mutual capacitance between the heatsink and the septum was obtained using (1). The measurement

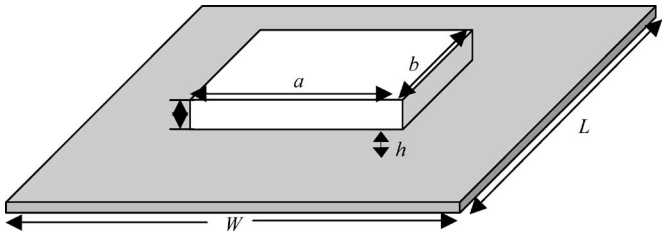

Fig. 11. Illustration of a heatsink test board.

TABLE II
MEASURED AND NUMERICALLY CALCULATED MUTUAL CAPACITANCE FOR HEATSINKS IN TEM CELL

Heatsink	# 1	# 2
Heatsink Dimensions (mm)	h = 19 a = 20 b = 20 t = 6.5	h = 22 a = 33 b = 31 t = 14
Measured C_{TEM} result (pF)	0.86	2.60
Simulated C_{TEM} result (pF)	0.76	2.58

was then repeated for another test board with a heatsink of different size. The two measurement results are compared with the corresponding results calculated using the quasi-static field solver in Table II. The measurement results and the numerically calculated results agree within 1 dB for both heatsink geometries.

In order to demonstrate that (4) can be used to estimate the self-capacitance of a heatsink from the mutual capacitance measured in a TEM cell, the self-capacitance of various heatsink geometries was calculated using a quasi-static field solver. These results were compared to the self-capacitances obtained by using the simulations of the heatsink in a TEM cell to obtain $C_{\rm TEM}$ and then applying (4). The self-capacitance values obtained using both of these techniques is shown in Fig. 12. For the curves labeled "various heights," a 30 mm × 30 mm × 10 mm heatsink was located at heights from 1 to 10 mm above the test board. For the curves labeled "various thicknesses," the heatsink was 30 mm long, 30 mm wide, and 2.4 mm above the test board, and the thickness varied from 2 to 20 mm. For the two curves labeled "Various lengths," the heatsink was 30 mm wide, 5 mm thick, and 2.4 mm above the test board, while the length varied from 10 to 50 mm. For all of the heatsink geometries investigated, the estimated self-capacitance values obtained from the TEM cell simulation and (4) agree with the full-wave simulation results within 1 dB.

B. Heatsink Radiated Emissions

To show that TEM cell measurements can be used to estimate the peak radiated emissions, the radiated emissions from a test board with a heatsink were measured in a semianechoic chamber, as shown in Fig. 13, and compared with the results derived from TEM cell measurements. The board was located 3 m away from the receiving antenna, and the signal driving the

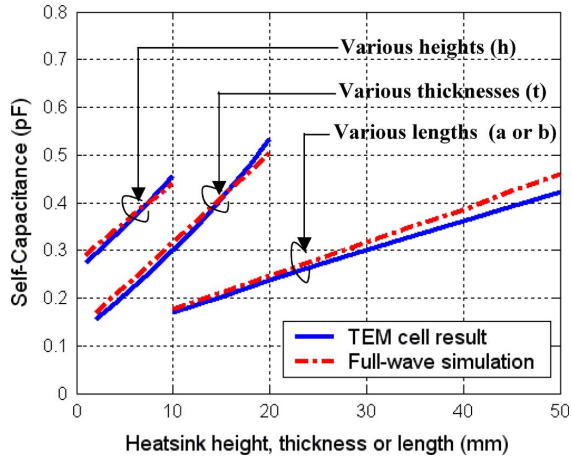

Fig. 12. Self-capacitance for various heatsink geometries.

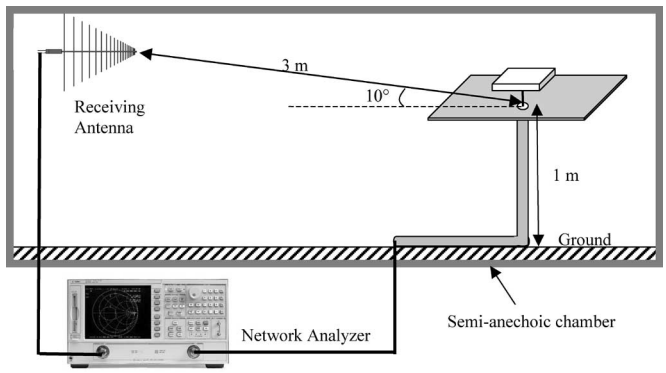

Fig. 13. Setup for radiated emissions measurement.

heatsink was delivered through a cable attached to the back side of the board near the middle. The board was 10 cm × 10 cm. The heatsink was 33 mm × 31 mm × 14 mm, and was 22 mm above the board. The peak voltage between the heatsink and the test board V_{DM} was 0 dBm (0.224 V). S_{21} results were converted to radiated field strengths using the equation

$$\mathrm{E}(\mathrm{dB}\mu\mathrm{V/m}) = V_{DM}(\mathrm{dB}\mu\mathrm{V}) + \mathrm{AF}(\mathrm{dB/m}) + S_{21}(\mathrm{dB}) \quad (9)$$

where AF is the antenna factor of the receiving antenna. The radiated emissions were also calculated using a full-wave electromagnetic field solver.[1] Fig. 14 plots the measured and simulated open-field radiated emissions.

In the frequency range investigated (30 to 250 MHz), the 10 cm × 10 cm board is electrically small and the self-capacitance of the heatsink is smaller than that of the board; therefore, the voltage-driven radiation model shown in Fig. 3 can be used to estimate the peak radiated emissions from the board with attached cables. The amplitude of the common-mode voltage source V_{CM} can be approximated as [9]

$$V_{CM} \approx \frac{C_{\rm heatsink}}{C_{\rm board}} V_{DM} \quad (10)$$

where $C_{\rm heatsink}$ is the self-capacitance of the heatsink, $C_{\rm board}$ is the self-capacitance of the board, and V_{DM} is the voltage

[1]CST Computer simulation technology, CST microwave studio 5.1.

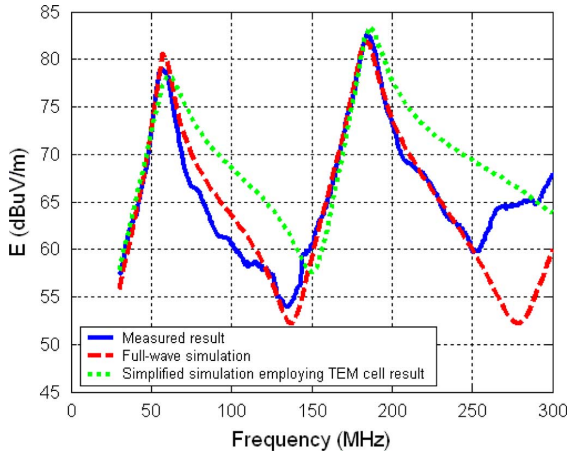

Fig. 14. Comparison of the radiated emissions from the chamber measurement, the full-wave simulation of the complete setup, and the corresponding simplified simulation using the measured self-capacitance.

between the heatsink and the board. V_{DM} and C_{heatsink} can be obtained from the TEM cell measurements using (7) and (4), respectively. The value of C_{board} can be estimated using the equation [14]

$$C_{\text{board}} \approx 8\varepsilon_0 \sqrt{\frac{\text{Board Area}}{\pi}}. \tag{11}$$

For this test board

$$V_{CM} = \frac{C_{\text{heatsink}}}{C_{\text{board}}} V_{DM} = \frac{1.23\ pF}{4.15\ pF} \times 0.224\ V = 0.066\ V. \tag{12}$$

With this information, the simulation of peak far-field radiation can be simplified by replacing the heatsink structure with an equivalent common-mode source V_{CM} between the board and the cable as described in [9].

The simulation results for the simplified structure are also shown in Fig. 14. The frequencies where the emissions are minimum are shifted due to the fact that the simple model puts the source in a different location. The minimum values occur at frequencies where the source location corresponds to a null in the current. The peak values occur at frequencies where the structure is resonant and are relatively independent of the source location. It is the peak emissions that are generally of interest. At the two peak frequencies, the results from the measurement, the full simulation, and the simplified simulation agree within 3 dB.

V. Conclusion

A previous study showed that electric field coupling from electrically small structures on PCBs can be modeled with simple ideal voltage sources and equivalent mutual capacitances. This paper demonstrates how TEM cell measurements can be used to determine these voltages and capacitances (or their products) and, therefore, characterize the electric-field coupling to cables and objects off the board. The proposed method involves connecting both outputs of the TEM cell to a hybrid in order to separate the electric field coupling from the magnetic field coupling. The product of the effective open-circuit voltage V_{DM} of an IC source and the source's self capacitance can be obtained directly from the hybrid TEM cell measurement. These results can then be used to predict the peak radiated emissions due to electric-field coupling from the traces, ICs, and heatsinks, without the need for modeling every detail of the source structure.

The frequency range of the TEM cell measurement is limited by the dimensions of the source and the TEM cell. For small ICs tested in a standard TEM cell, the upper frequency limit is 1 GHz. The model used to predict the maximum radiated emissions from the cable is valid at frequencies where the PCB is electrically small. For the 10 cm square board in the example presented here, the upper frequency limit was about 250 MHz. In most cases, the frequency range of the TEM cell measurement is more than sufficient to characterize the device coupling that results in significant cable radiation.

References

[1] *Measurement of Radiated Emissions from Integrated Circuits—TEM/Wideband TEM (GTEM) Cell Method; TEM Cell (150 kHz to 1 GHz), Wideband TEM Cell (150 kHz to 8 GHz)*, Soc. Autom. Eng. Standard SAE J1752/3, Jan. 2003.

[2] *Integrated Circuits—Measurement of Electromagnetic Emissions, 150 kHz to 1 GHz—Part 2: Measurement of Radiated Emissions, TEM-Cell and Wideband TEM-Cell Method*, Int. Electrotech. Commiss. Standard IEC 61967–2:2005, First edition, Sep. 2005.

[3] V. Kasturi, S. Deng, T. Hubing, and D. Beetner, "Quantifying electric and magnetic field coupling from integrated circuits with TEM cell measurements," in *Proc. 2006 IEEE Int. Symp. Electromagn. Compat.*, Portland, OR, Aug. 14–18, pp. 422–425.

[4] A. Nakamura, "EMC Basic Series No. 21: Measurement methods and applications of electromagnetic emission of semiconductor devices," *J. Jpn. Inst. Electron. Packag.* (in Japanese), vol. 6, no. 4, pp. 344–351, 2004.

[5] D. Hockanson, J. Drewniak, T. Hubing, T. Van Doren, F. Sha, and M. Wilhelm, "Investigation of fundamental EMI source mechanisms driving common-mode radiation from printed circuit boards with attached cables," *IEEE Trans. Electromagn. Compat.*, vol. 38, no. 4, pp. 557–566, Nov. 1996.

[6] G. Dash, J. Curtis, and I. Straus, "The current driven model—Experimental verification and the contribution of Idd delta to digital device radiation," in *Proc. 1999 IEEE Int. Symp. Electromagn. Compat.*, Seattle, WA, Aug. 1999, pp. 317–322.

[7] R. Dockey and R. German, "New techniques for reducing printed circuit board common-mode radiation," in *Proc. 1993 IEEE Int. Symp. Electromagn. Compat.*, Dallas, TX, Aug. 1993, pp. 334–339.

[8] M. Leone, "Design expressions for trace-to-edge common-mode inductance of a printed circuit board," *IEEE Trans. Electromag. Compat.*, vol. 43, no. 4, pp. 667–671, Nov. 2001.

[9] H. W. Shim and T. H. Hubing, "Model for estimating radiated emissions from a printed circuit board with attached cables driven by voltage-driven sources," *IEEE Trans. Electromag. Compat.*, vol. 47, no. 4, pp. 899–907, Nov. 2005.

[10] Ansoft Corporation, *Q3D Extractor Version 7.0 User's Guide*. Pittsburgh, PA: Ansoft Corp., Aug. 2005.

[11] F. Schnieder and W. Heinrich, "Model of thin-film microstrip for circuit design," *IEEE Trans. Microw. Theory Tech.*, vol. 49, no. 1, pp. 104–110, Jan. 2001.

[12] K. C. Gupta, R. Garg, and I. Bahl, *Microstrips and Slot Lines*, 2nd ed. Norwood, MA: Artech House, 1996.

[13] H. W. Shim and T. H. Hubing, "Derivation of a closed-formed approximate expression for the self-capacitance of a printed circuit board trace," *IEEE Trans. Electromagn. Compat.*, vol. 47, no. 4, pp. 1004–1008, Nov. 2005.

[14] S. Alan Roy, "Simulation tools for the analysis of single electronic systems," Ph.D. Thesis, Dept. Electron. Elect. Eng., Univ. Glasgow, Glasgow, U.K., 1994.

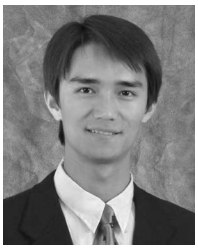

Shaowei Deng was born in Nanchang, China, in 1979. He received the B.S. degree in electrical engineering from Fudan University, Shanghai, China, in 2001, and the M.S. and Ph.D. degrees in electrical engineering from the University of Missouri–Rolla, Rolla, in 2002 and 2007, respectively.

He is currently with Juniper Networks in Sunnyvale, CA.

Todd Hubing (S'82–M'82–SM'93–F'06) received the B.S.E.E. degree in electrical engineering from the Massachusetts Institute of Technology, Cambridge, in 1980, the M.S.E.E. degree in electrical engineering from Purdue University, West Lafayette, IN, in 1982, and the Ph.D. degree in electrical engineering from North Carolina State University, Raleigh, in 1988.

From 1982 to 1989, he was with the Electromagnetic Compatibility Laboratory, International Business Machines (IBM) Communications Products Division, Research Triangle Park, NC. In 1989, he became a Faculty Member at the University of Missouri–Rolla (UMR), Rolla, where he worked to analyze and develop solutions for a wide range of electromagnetic compatibility problems affecting the electronics industry. In 2006, he joined Clemson University, Clemson, SC, as the Michelin Professor for Vehicular Electronics. His current research interests include electromagnetic compatibility and computational electromagnetic modeling, particularly as it is applied to automotive and aerospace electronics.

Prof. Hubing was an Associate Editor of the IEEE TRANSACTIONS ON ELECTROMAGNETIC COMPATIBILITY, the IEEE ELECTROMAGNETIC COMPATIBILITY SOCIETY NEWSLETTER, and the *Journal of the Applied Computational Electromagnetics Society*. From 2002 to 2003, he was the President of the IEEE Electromagnetic Compatibility Society and continues to be on the Society's Board of Directors.

Daryl G. Beetner (S'89–M'98–SM'03) received the B.S. degree in electrical engineering from Southern Illinois University, Edwardsville, in 1990, and the M.S. and D.Sc. degrees in electrical engineering from Washington University, St. Louis, MO, in 1994 and 1997, respectively.

He is currently an Associate Professor of electrical and computer engineering at the University of Missouri—Rolla, Rolla, where he is also the Associate Chair of the Computer Engineering Program. His current research interests include electromagnetic compatibility, very large scale integrated circuit design, skin cancer detection, and detection of electronics and explosive devices.